JOURNAL OF SOLID STATE CHEMISTRY 103, 114–130 (1993)

Synthesis, Characterization, and Bonding of Indium Cluster Phases: $Na_{15}In_{27.4}$, a Network of In_{16} and In_{11} Clusters; Na_2In with Isolated Indium Tetrahedra

SLAVI C. SEVOV AND JOHN D. CORBETT

Ames Laboratory–DOE[1] and the Department of Chemistry, Iowa State University, Ames, Iowa 50011

Received May 21, 1992; accepted August 10, 1992

The remaining phases in the Na–In system have been identified and characterized. The indium-richest is $Na_{15}In_{27.4}$, with a structure containing novel *closo*-In_{16} clusters interconnected to two kinds of *nido*-In_{11} units and isolated, 4-bonded atoms (*Cmcm*, $Z = 8$, $a = 16.108$ (4) Å, $b = 35.279$ (8) Å, $c = 15.931$ (3) Å, $R/R_w = 0.041/0.044$ at the indium-rich limit $Na_{15}In_{27.54}$). Fractional occupancy of two atoms in cluster chain positions were found, one as a function of a narrow nonstoichiometry. The structure is related to that recently established for $Na_7In_{11.8}$. Resistivity and magnetic properties are consistent with a small (0.5–3.2%) excess of electrons relative to the calculated bonding requirements. The sodium-richest phase is the stable, diamagnetic, and weakly metallic Na_2In, isostructural with Na_2Tl ($C222_1$, $Z = 16$, $a = 13.855$ (1) Å, $b = 8.836$ (1) Å, $c = 11.762$ (1) Å, $R/R_w = 0.030/0.034$). A corrected phase diagram is given.

Introduction

Knowledge of the binary Na–In system has been quite limited. The present phase diagram (1, 2) is based largely on thermal analysis (3, 4) and indicates a congruently melting phase at approximately Na_5In_8 or Na_2In_3, the Zintl phase NaIn (NaTl-type) (5), and a sodium-rich member Na_3In (3) or Na_2In (4). We have already reported on the structure and properties of $Na_7In_{11.8}$, the maximum melting compound (6). While exploring the region of stoichiometries over which this compound is stable, we observed that a second phase is formed on the indium-richer side. This article reports on this compound, namely, $Na_{15}In_{27.4}$ (35.4 at.% Na), which exhibits a network structure closely related to that in $Na_7In_{11.8}$. We also discuss the identification and properties of Na_2In, the sodium-richest phase in the system.

Experimental

Syntheses

The reagents and the reaction techniques in welded tantalum tubing were described before (6). All materials were handled in a N_2-filled glovebox.

Composition space in Na–In was further explored following our identification and

[1] The Ames Laboratory–DOE is operated for the U.S. Department of Energy by Iowa State University under Contract W-7405-Eng-82. This research was supported by the Office of Basic Energy Sciences, Materials Sciences Division. The U.S. Government's right to retain a nonexclusive royalty-free license in and to the copyright covering this paper, for governmental purposes, is acknowledged.

0022-4596/93 $5.00

characterization of $Na_7In_{11.76}$ (37.3 at.% Na) as well as observation of the well-known NaIn (50.0% Na). Compositions of 35 and 67% Na were melted at 550°C and then slowly cooled to room temperature at 5°C per hr. (The liquidus temperatures for these are at about 440 and 330°C, respectively (1).) The products were metallic in appearance and very brittle. Both samples react with moist air rapidly, with bubbling; in no way to any of these exhibit the air stability reported for the maximum melting "Na_2In_3" (3). Single crystals of $Na_{15}In_{27.54}$ (35.3% Na) and Na_2In (66.7%) were obtained from the respective samples.

Powder patterns were obtained after grinding the samples and mounting the powder between pieces of cellophane tape. An Enraf–Nonius Guinier camera, Cu $K\alpha$ radiation (λ = 1.540562 Å) and NBS (NIST) silicon as an internal standard were employed for this purpose. Patterns of the above phases were later indexed with the aid of patterns calculated on the basis of the refined structures. Least-square refinements for 29 lines from the $Na_{15}In_{27.5}$ phase limit and 35 lines from Na_2In afforded the lattice constants a = 16.108 (4) Å, b = 35.279 (8) Å, and c = 15.931 (3) Å for $Na_{15}In_{27.5}$ and a = 13.855 (1) Å, b = 8.836 (1) Å, and c = 11.762 (1) Å for Na_2In. Errors for the former are somewhat large because this particular combination of a large cell and near-tetragonality produce many diffraction lines, and these are often grouped very close to one other, making their measurement and assignment rather ambiguous at times.

A reaction designed to produce the reported Na_3In was carried out at that composition and under the reaction conditions described above. The product by eye clearly contained unreacted sodium metal, but many small crystallites could be seen in the soft matrix. The X-ray powder pattern showed the presence of NaIn, Na_2In, and Na. The sample was sealed in a Pyrex ampoule under vacuum and equilibrated at 140°C for 10 days. This time the amounts of NaIn and Na seen by powder pattern were negligible compared with that of Na_2In. A second equilibration was made at 240°C for 10 days, above what we conclude is the peritectic decomposition temperature of Na_2In (see Phase Diagram), and the sample quenched. If Na_2In existed up to 286°C, as in one proposal (4), it should have been seen in this product, but only NaIn and Na with traces of Na_2In were evident in the powder pattern. No evidence of either a peritectic decomposition point of 96°C for "Na_3In" (3) or of a suggested lower (peritectoid) stability limit for Na_2In at 160°C (4) could be found, either in the initial Na_3In reaction above which was cooled to room temperature at 5°C hr^{-1} or after an equilibration of the Na_2In in that sample for 14 days at 90°C. The "Na_3In" composition assignment was based on direct analysis and must have resulted from the virtual inseparability of Na and Na_2In by physical means.

Nonstoichiometry

A change in the occupancy of the In19 position in the $Na_{15}In_{27.54}$ structure (below) over a range of compositions was thought possible. Therefore, additional reactions with both 20 and 36.8 at.% Na were carried out. The former was treated as first described while the latter was heated at 490°C for 2 hr and then at 410°C and 250°C for 3 and 5 days, respectively.

The indium-richer sample provided the $Na_{15}In_{27.4}$ phase and a lot of unreacted indium metal, proving that the former is the indium-richest compound in the system. The lattice parameters of the former phase, a = 16.129 (3) Å, b = 35.308 (6) Å, and c = 15.952 (2) Å), differ by only +4, +3, and +6σ, respectively, from the values obtained earlier for the sample used for the structure refinement, indicating that the refined composition (below) is close to upper indium limit. (Higher occupancy of the

fractional In19 position therein would cause a significant expansion of the *c*-axis—see Structural Descriptions.) The other reaction produced the known $Na_7In_{11.76}$ (37.3 at.% Na) as a major phase, but lines from the $Na_{15}In_{27.4}$ structure could also be measured, and these gave a = 16.119 (3) Å, b = 35.141 (7) Å, and c = 15.945 (4) Å. These demonstrate a significant contraction of the *b*-axis at the indium-poor limit (0.167 Å, 18σ), while the *a*- and *c*-axes remain about the same (<3σ differences). A second structural study was therefore carried out on this sample to clarify this point, since reduced occupation of a site other than that of In19 was implied.

Structure Determinations

Three sets of diffraction data were collected at room temperature on CAD4 single-crystal diffractometer with monochromated Mo $K\alpha$ radiation ($2\theta_{max}$ = 50°), and the structures were refined with the aid of the TEXAN package (7). Some details of the data collection and refinement are listed in Table I. Unique aspects of the crystallography follow:

$Na_{15}In_{27.54}$. A few wedge-shaped pieces picked from the crushed sample were sealed in thin-walled glass capillaries and checked by means of oscillation, Weissenberg, and precession photographs for quality and, eventually, a space group assignment. The photographs showed a C-centered orthorhombic cell with additional systematic absences consistent with three possible space groups—*Cmcm* (no. 63), $Cmc2_1$ (no. 36), and *C2cm* (no. 40, nonstd.). A crystallite ca. 0.3 × 0.1 × 0.07 mm was chosen, and 25 reflections from a random search by the diffractometer were indexed with a C-centered orthorhombic cell of the expected dimensions. One octant of data was collected with no imposed conditions. The possible space groups were confirmed after corrections for Lorentz and polarization effects, as well as for absorption with the aid of the average of three ψ-scans at different θ values. Only a few relatively weak reflections ($I/\sigma(I) \sim 3$) violated the C-centering. The Wilson plot clearly suggested a centrosymmetric space group, and thus *Cmcm* was chosen for the first trial.

TABLE I

SELECTED DATA COLLECTION AND REFINEMENT PARAMETERS FOR $Na_{15}In_{27.54}$ AND Na_2In

Formula	$Na_{15}In_{27.54}$	Na_2In
Space group	*Cmcm*	$C222_1$
Z	8	16
a (Å)[a]	16.108 (4)	13.855 (1)
b (Å)	35.279 (8)	8.836 (1)
c (Å)	15.931 (3)	11.762 (1)
V (Å^3)	9053 (6)	1440 (4)
Crystal dimensions (mm)	0.07 × 0.1 × 0.3	0.1 × 0.1 × 0.2
$2\theta_{max}$ (deg.)	50	50
Scan mode	ω-θ	ω-θ
Octants	h, k, l	$\pm h, k, l$
Reflections		
Measured	8733	2683
Observed	2252	2054
Independent	2252	999
μ (Mo $K\alpha$), cm^{-1}	137.4	64.2
Trans. coeff. range	0.910–1.06	0.858–1.08
R_{ave} (all data) (%)	—	5.6
R^b (%)	4.1	3.0
$R_w{}^c$ (%)	4.4	3.4

[a] *Guinier data.*
[b] $R = \Sigma\|F_o| - |F_c\|/\Sigma|F_o|$.
[c] $R_w = [\Sigma w(|F_o| - |F_c|)^2/\Sigma w(F_o)^2]^{1/2}$; $w = [\sigma(F)]^{-2}$.

Application of direct methods (8) gave 19 positions with distances around each appropriate to indium. The weight of one of these was approximately half of the average of the others, and so only the 18 larger positions were assigned as In for the first few least-squares cycles. A subsequent difference-Fourier synthesis again revealed the position in question together with 14 others, the latter having appropriate distances for sodium atoms. The odd peak was approximately twice the average height of the sodium positions, and so it was assigned as indium (In19). Refinement with isotropic thermal parameters led to R = 9.8% and to an unreasonably large thermal parameter for In19. Consequently this atom

was refined with partial occupancy, 54.1(9)% in the final analysis. The occupancies of the other In atoms did not deviate from unity by more than 4% (3–4σ) when the Na atoms were kept fixed, and of Na, by 5–8% (~3σ) when the In atoms were fixed. Therefore, these other occupancies were all held at unity in the final refinement. The final residuals were R(F) = 4.1%, R_w = 4.4% with variation of positions, anisotropic thermal parameters and the multiplicity of In19 after application of DIFABS for an empirical absorption correction (9). The refined composition is $Na_{15}In_{27.541(9)}$ (35.26 (2) at.% Na). The largest residual peaks in the final difference Fourier map were 1.6 e/Å^3 (1.9 Å from In7) and −2.3 e/Å^3.

The facts that In19 refines with occupancy within 4σ of 50% and that the distance to an equivalent position generated by the center of symmetry—2.76 (1) Å—is significantly shorter than the shortest distance observed in $Na_7In_{11.8}$—2.845 (5) Å—suggested that the structure might be acentric in only this respect. Consequently, the $Cmc2_1$ group was assigned, and atomic positions calculated from the refined coordinates in *Cmcm*. In19 was placed at one of the two possible positions. (This nonetheless seemed unlikely as linear chains of *nido*-icosahedra running along the *c*-axis (see structure description) and all facing one way would make the crystal polar.) However, a difference-Fourier map contained the other peak with a considerable height. The result was the same when the other enantiomorph was used. Not surprising, attempts to refine the structure as acentric led to a very pronounced coupling between parameters of pairs of equivalent atoms in *Cmcm*. Film work excluded the possibility of a superlattice along **c**. All these results were interpreted as evidence that the structure has a center of symmetry, and the In19 position is randomly occupied.

In order to establish the nature of the apparent nonstoichiometry of $Na_{15}In_{27.4}$, diffraction data were collected from a single crystal picked from the sample at the indium-poor limit (see above).[2] The final positional and thermal parameters (available from J.D.C.) as well as interatomic distances were very close to those for $Na_{15}In_{27.54}$ (within 5σ) except for some larger changes associated with the smaller *b*-axis. The major difference is the partial occupancy of the In15 site (64.4 (7)%) in addition to that of In19 (51.5 (7)%). The corresponding composition is $Na_{15}In_{27.16(1)}$ (35.6 at.% Na). The occupancy of In19 is again very close to one-half and within 3σ of that at the indium-rich limit.

Na_2In. Some single crystals without a particular shape were sealed in capillaries and checked for singularity by oscillation photographs. One of them (ca. 0.2 × 0.1 × 0.1 mm) was selected, and 25 reflections from the random search were indexed with a C-centered orthorhombic cell. Two octants of data were collected with the appropriate absence condition imposed. The diffraction data were corrected for Lorentz and polarization effects and also for absorption with the aid of ψ-scans of three reflections. The output showed an additional systematic extinction condition consistent with only one space group—$C222_1$ (no. 20). Direct methods gave two positions that were assigned to indium in the starting model. A few least-squares cycles and a difference-Fourier map gave five more positions with distances to the indium atoms appropriate for sodium, and they were so assigned. Refinement with isotropic thermal parameters proceeded smoothly, and a DIFABS empirical absorption correction was applied after convergence. Occupan-

[2] Two octants of data were collected with the absence condition for C-centering imposed. Results were R_{ave} = 5.5% (all data), R(F), R_w = 3.9, 5.0% for 2734 independent reflections, 229 variables and with absorption (μ = 134.3 cm^{-1}) corrected as before.

cies deviated from unity by $< 2\sigma$. The final residuals after anisotropic refinement of all atoms were $R = 3.0\%$, $R_w = 3.4\%$. No peaks larger than 1 e/Å^3 appeared in the final difference-Fourier map. The result was later recognized as the Na_2Tl structure (10). (Structure factor data as well as anisotropic displacement parameters for both structures are available from J.D.C.)

Property Measurements

The electrical resistivities of the two compounds were again measured by an electrodeless "Q" method (11). These utilized a sized, powdered sample mixed with chromatographic Al_2O_3 and were made at 34 MHz and every 10° between 130 and 295 K. Sample magnetizations were measured at 3 Tesla over the range 6-295 K on a Quantum Design MPMS SQUID magnetometer. The raw data were corrected for the susceptibilities of the containers. The diamagnetic correction procedures are described in more detail elsewhere (6).

TABLE II

POSITIONAL PARAMETERS AND B_{eq} FOR $Na_{15}In_{27.5}$

Atom	Posn.	x	y	z	B_{eq}
In1	8*g*	0.0895(1)	0.17207(6)	1/4	1.2(1)
In2	16*h*	0.1854(1)	0.11231(4)	0.1561(1)	1.23(6)
In3	8*g*	0.3486(2)	0.09527(7)	1/4	1.4(1)
In4	16*h*	0.1819(1)	0.19304(4)	0.0934(1)	1.33(7)
In5	16*h*	0.0930(1)	0.21236(4)	−0.0600(1)	1.43(7)
In6	16*h*	0.3482(1)	0.14358(4)	0.0967(1)	1.46(7)
In7	16*h*	0.3182(1)	0.04888(5)	−0.1545(1)	1.84(7)
In8	16*h*	0.3405(1)	0.22383(4)	0.1572(1)	1.39(7)
In9	16*h*	0.4059(1)	0.11170(5)	−0.0665(1)	2.01(8)
In10	8*f*	0	0.15108(6)	−0.1556(1)	1.5(1)
In11	8*g*	0.4087(2)	0.01440(6)	1/4	1.7(1)
In12	8*g*	0.1736(2)	0.24970(7)	1/4	1.6(1)
In13	16*h*	0.0915(1)	0.05374(5)	0.0788(1)	2.13(8)
In14	16*h*	0.1547(1)	0.02509(5)	−0.0850(1)	2.28(8)
In15	8*f*	0	0.47589(8)	0.0794(2)	3.0(1)
In16	8*g*	0.1691(2)	0.36395(8)	1/4	2.9(1)
In17	8*f*	0	0.07440(7)	−0.0862(2)	2.4(1)
In18	8*f*	0	0.67349(7)	−1594(2)	2.7(1)
In19[a]	8*f*	0	−0.0035(1)	0.1635(3)	2.1(2)
Na1	4*c*	0	0.4180(3)	1/4	1.9(5)
Na2	4*c*	0	0.6636(5)	1/4	1.9(9)
Na3	16*h*	0.3129(7)	0.0431(3)	0.0602(6)	2.6(5)
Na4	4*c*	0	0.0876(6)	1/4	3.0(10)
Na5	8*f*	0	0.1435(3)	0.0595(9)	2.0(6)
Na6	8*f*	0	0.5794(4)	0.1127(9)	2.3(6)
Na7	8*g*	0.134(1)	−0.0844(4)	1/4	2.9(7)
Na8	16*h*	0.1932(7)	0.1222(3)	0.5598(6)	2.5(5)
Na9	8*f*	0	0.2382(4)	0.129(1)	2.7(7)
Na10	8*f*	0	0.6988(4)	0.0370(8)	2.1(6)
Na11	8*g*	0.1723(8)	−0.1869(4)	1/4	2.3(6)
Na12	8*g*	0.2036(8)	0.0242(4)	1/4	2.1(6)
Na13	16*h*	0.3121(6)	0.2084(3)	0.5695(6)	2.8(5)
Na14	4*c*	0	−0.2375(6)	1/4	3.0(10)

[a] Occupancy = 54.1(9)%, giving the composition $Na_{15}In_{27.541(9)}$.

Structure Descriptions

$Na_{15}In_{27.4}$

This phase exhibits a small homogeneity range corresponding to about ±0.2 in the indium coefficient. The phase is referred to by its mean composition unless changes therewith are important.

The final positional and isotropic-equivalent displacement parameters and the important distances at the indium-rich $Na_{15}In_{27.54}$ limit are listed in Tables II and III, respectively. The general view of the unit cell in Fig. 1 outlines all In–In distances less than 3.5 Å.

The structure can be described as a network of four types of clusters: 12-bonded *closo*-icosioctahedra (In_{16}) (that is, with 12 exo-bonds to other cluster units), 10-bonded *nido*-icosahedra (In_{11}, denoted as type A hereafter), 10-, 11-, or 12-bonded *closo*-, *nido*-, or *arachno*-icosahedra (In_{12}, In_{11}, or In_{10}, type B hereafter), depending on the interpretation of the fractional occupancy of In19, and 6-bonded In_3 triangles.

The novel 16-vertex cluster has C_{2v} ($m2m$) point group symmetry (Fig. 2a). The first example of such a species (although 8-bonded) was found in $Na_7In_{11.8}$. The cluster can be described as a tetracapped truncated tetrahedron, the capping atoms (pairs of In15 and 16) being 6-bonded while the rest (In7, 9, 11, 18) are 5-bonded within the cluster. All but In16 and In18 also have exo-bonds; In7 and In9 (4 of each) and the pair of In12 thus bond the cluster to 10 different In_{11} while the In15 pair are bonded to In15 in two other such In_{16} clusters (Figs.

TABLE III

Distances of Nearest Neighbors about Each Atom in $Na_{15}In_{27.54}$[a]

In1

	In1	2.882(5)
2	In2	3.012(3)
2	In4	2.999(2)
	In12	3.055(3)
	Na4	3.31(2)
2	Na5	3.51(1)
2	Na9	3.35(1)

In2

	In1	3.012(3)
	In2	2.983(3)
	In3	3.085(3)
	In4	3.019(2)
	In6	2.998(3)
	In13	2.841(2)
	Na3	3.54(1)
	Na4	3.452(6)
	Na5	3.535(7)
	Na8	3.46(1)
	Na12	3.46(1)

In3

2	In2	3.085(3)
2	In6	2.979(2)
	In11	3.012(3)
	Na2	3.43(1)
2	Na3	3.59(1)
2	Na6	3.32(1)
	Na12	3.43(1)

In4

	In1	2.999(2)
	In2	3.019(2)
	In5	2.913(2)
	In6	3.198(3)
	In8	2.957(2)
	In12	3.200(2)
	Na5	3.453(7)
	Na8	3.50(1)
	Na9	3.383(7)
	Na13	3.38(1)
	Na13	3.500(9)

In5

	In4	2.913(2)
	In5	2.996(3)
	In8	2.935(2)
	In10	3.039(3)
	Na5	3.43(1)
	Na8	3.57(1)
	Na9	3.49(1)
	Na10	3.49(1)
	Na11	3.406(6)
	Na13	3.53(1)
	Na13	3.80(1)
	Na14	3.492(6)

In6

	In2	2.998(3)
	In3	2.979(2)
	In4	3.198(3)
	In8	2.993(2)
	In9	2.982(2)
	Na2	3.528(4
	Na3	3.638(9)
	Na6	3.34(1)
	Na8	3.61(1)
	Na10	3.268(9)
	Na13	3.546(9)

In7

	In7	3.042(3
	In9	2.979(2)
	In11	3.070(3)
	In14	2.978(3)
	In15	3.283(2)
	In16	3.437(3)
	Na1	3.501(4
	Na3	3.427(9)
	Na3	3.577(9)
	Na7	3.56(1)
	Na8	3.61(1)
	Na12	3.52(1)

In8

	In4	2.957(2)
	In5	2.935(2)
	In6	2.993(2)
	In8	2.956(3)
	In12	3.202(3)
	Na2	3.65(1)
	Na10	3.324(1)
	Na11	3.48(1)
	Na13	3.68(1)
	Na13	3.70(1)
	Na14	3.262(9)

In9

	In6	2.982(2)
	In7	2.979(2)
	In9	3.033(4)
	In15	3.448(3)
	In16	3.277(2)
	In18	3.040(3)
	Na1	3.456(4)
	Na3	3.49(1)
	Na6	3.43(1)
	Na8	3.45(1)
	Na10	3.80(1)
	Na13	3.73(1)

In10

2	In5	3.039(3)
	In10	3.007(5)
	In17	2.923(3)
	Na5	3.44(1)
2	Na7	3.53(1)
2	Na8	3.61(1)
2	Na11	3.40(1)
	Na14	3.40(2)

In11

	In3	3.012(3)
2	In7	3.070(3)
	In11	2.943(5)
2	In15	3.377(3)
	Na1	3.71(1)
2	Na3	3.54(1)
2	Na6	3.49(1)
	Na12	3.32(1)

In12

	In1	3.055(3)
2	In4	3.200(2)
2	In8	3.202(3)
	In16	*4.032(4)*
2	*In18*	*4.152(3)*
2	Na9	3.418(9)
	Na11	3.34(1)
2	Na13	3.242(9)

In13

	In2	2.841(2)
	In13	2.948(4)
	In14	2.978(3)
	In14	2.963(2)
	In17	3.100(3)
	In19	2.841(5)
	Na3	3.60(1)
	Na4	3.323(8)
	Na5	3.51(1)
	Na8	3.66(1)
	Na12	3.433(8)

In14

	In7	2.978(3)
	In13	2.978(3)
	In13	2.963(2)
	In14	3.236(4)
	In17	3.039(2)
	In19	2.889(3)
	Na3	3.50(1)
	Na3	3.53(1)
	Na7	3.375(9)
	Na8	3.51(1)
	Na12	3.248(8)

In15

2	In7	3.283(2
2	In9	3.448(3)
2	In11	3.377(3)
	In15	3.047(6)
	Na1	3.400(7
2	Na3	3.80(1)
2	Na3	3.85(1)
	Na6	3.69(1)
	Na6	3.63(2)

In16

2	In7	3.437(3)
2	In9	3.277(2)
2	In18	3.353(3)
	Na1	3.325(7)
	Na7	3.66(2)
2	Na8	3.79(1)
	Na11	3.12(1)
2	Na13	3.86(1)

In17

	In10	2.923(3)
2	In13	3.100(3)
2	In14	3.039(2)
	In19	2.788(6)
	Na5	3.37(1)
2	Na7	3.40(1)
2	Na8	3.57(1)

In18

2	In9	3.040(3)
2	In16	3.353(3)
	In18	2.885(5)
	Na1	3.54(1)
	Na9	3.15(1)
	Na10	3.25(1)
2	Na13	3.57(1)

In19

2	In13	2.841(5)
2	In14	2.889(3)
	In17	2.788(6)
	In19	2.760(10)
	Na4	3.50(2)
2	Na7	3.83(2)
2	Na12	3.69(1)

TABLE III—*Continued*

Na1		**Na5**		**Na8**		**Na11**	
4	In7	3.501(4)	2	In1	3.51(1)		In2	3.46(1)	2	In5	3.406(6)
4	In9	3.456(4)	2	In2	3.535(7)		In4	3.50(1)	2	In8	3.48(1)
2	In11	3.71(1)	2	In4	3.453(7)		In5	3.57(1)	2	In10	3.40(1)
2	In15	3.400(7)	2	In5	3.43(1)		In6	3.61(1)		In12	3.34(1)
2	In16	3.325(7)		In10	3.44(1)		In7	3.61(1)		In16	3.12(1)
2	In18	3.54(1)	2	In13	3.51(1)		In9	3.45(1)			
				In17	3.37(1)		In10	3.61(1)		Na7	3.67(2)
Na2							In13	3.66(1)	2	Na8	3.81(1)
				Na4	3.62(2)		In14	3.51(1)	2	Na13	3.73(1)
2	In3	3.43(1)	2	Na8	3.72(1)		In16	3.79(1)		Na14	3.30(2)
4	In6	3.528(4)		Na9	3.51(2)		In17	3.57(1)			
4	In8	3.65(1)							**Na12**		
			Na6				Na3	3.89(1)	2	In2	3.46(1)
2	Na6	3.69(2)					Na5	3.72(1)		In3	3.43(1)
2	Na10	3.61(1)	2	In3	3.32(1)		Na7	3.45(1)	2	In7	3.52(1)
	Na14	3.49(3)	2	In6	3.34(1)		Na11	3.81(1)		In11	3.32(1)
			2	In9	3.43(1)		Na13	3.59(1)	2	In13	3.433(8)
Na3			2	In11	3.49(1)				2	In14	3.248(8)
				In15	3.69(1)		**Na9**		2	In19	3.69(1)
	In2	3.54(1)		In15	3.63(2)						
	In3	3.59(1)				2	In1	3.35(1)	2	Na3	3.56(1)
	In6	3.638(9)		Na2	3.69(2)	2	In4	3.383(7)		Na4	3.97(2)
	In7	3.427(9)	2	Na3	3.38(1)	2	In5	3.49(1)		Na7	3.99(2)
	In7	3.577(9)				2	In12	3.418(9)			
	In9	3.49(1)	**Na7**				In18	3.15(1)	**Na13**		
	In11	3.54(1)									
	In13	3.60(1)	2	In7	3.56(1)		Na5	3.52(2)		In4	3.38(1)
	In14	3.50(1)	2	In10	3.53(1)		Na9	3.85(3)		In4	3.500(9)
	In14	3.53(1)	2	In14	3.375(9)		Na10	3.46(2)		In5	3.53(1)
	In15	3.80(1)		In16	3.66(2)	2	Na13	3.69(1)		In5	3.80(1)
	In15	3.85(1)	2	In17	3.40(1)					In6	3.546(9)
			2	In19	3.83(2)	**Na10**				In8	3.68(1)
	Na3	3.59(2)								In8	3.70(1)
	Na6	3.38(1)	2	Na8	3.45(1)	2	In5	3.49(1)		In9	3.73(1)
	Na8	3.89(1)		Na11	3.67(2)	2	In6	3.268(9		In12	3.242(9)
	Na12	3.56(1)		Na12	3.99(2)	2	In8	3.324(8)		In16	3.86(1)
						2	In9	3.80(1)		In18	3.57(1)
Na4							In18	3.25(1)		Na8	3.59(1)
										Na9	3.69(1)
2	In1	3.31(2)					Na2	3.61(1)		Na10	3.49(1
4	In2	3.452(6)					Na9	3.46(2)		Na11	3.73(1)
4	In13	3.323(8)				2	Na13	3.49(1)			
2	In19	3.50(2)							**Na14**		
2	Na5	3.62(2)							4	In5	3.492(6)
2	Na12	3.97(2)							4	In8	3.262(9)
									2	In10	3.40(2)
										Na2	3.49(3)
									2	Na11	3.30

[a] Distance limits: In–In < 4.5 Å; In–Na < 4.55 Å; Na–Na < 4.05 Å.

2a, 3) to form zig-zag chains. Bonds within the cluster involving the 6-bonded In15 and In16 are characteristically longer (3.277 (2)–3.448 (3) Å) than between the rest (2.885 (5)–3.070 (3) Å), and the former exhibit larger thermal ellipsoids. In18 has the third largest ellipsoid, which probably derives from the lack of an exo-bonds to it. The In_{16} cluster is centered by the Na1 ion and is stoichiometric at the indium-rich

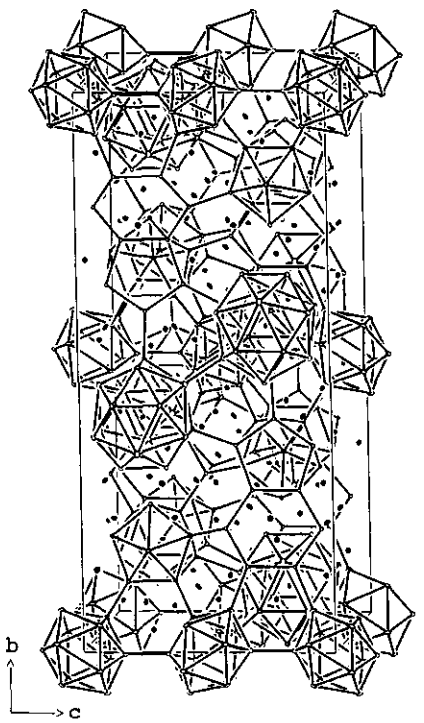

FIG. 1. A view of the unit cell of $Na_{15}In_{27.4}$ slightly off [100]. Lines connect all In atoms <3.5 Å apart, while Na atoms are shown as dots.

limit $Na_{15}In_{27.54}$, but In15 therein exhibits a 64.4 (7)% occupancy at the indium-poor limit $Na_{15}In_{27.16}$. The bonding at In15 is at this time unique, the first example of indium bonded to six atoms within the cluster plus an exo-bond as well. Partial and random occupancy of this site toward one limit means that some of the icosioctahedra will be *nido*-In_{15} and perhaps a few, *arachno*-In_{14} modifications, which are automatically only 11- or 10-bonded units. Since the In15–In15 bonds have components only along $[0,y,z]$, changes in the occupancy will only affect the *b*- and *c*-axes. Moreover, the length of the *c*-axis seems to be defined mainly by the chains of In_{11} units running along it (below), and the major effect of reduced In15 occupancy is an observed decrease in the *b*-axis as these chains flatten (see Experimental section).

There are two types of polyhedra derived from icosahedra in this structure. The first, type A, are 10-bonded *nido*-In_{11} (In1, 2, 3, 4, 6, 8, 12) with only *m* symmetry (Fig. 2b). The missing vertex is opposite to In1, and all atoms but In12 are exo-bonded. The A clusters are bonded back-to-back via In1–In1. The In3 and a pair of In6 atoms therein are bonded to three different In_{11} (all type A), the two In2 are bonded to two different In_{11} (type B, Fig. 2c), and In4 and 8 are bonded to different indium triangles (Figure 2d). Finally, In12, which lacks an exo-bond, has a position that can be described as remotely capping an open triangular face on a neighboring In_{16} cluster defined by two In18 and one In16 atoms, all of which also have no exo-bonds. This will be important later in electronic considerations.

The second In_{11}, type B, has C_{2h} (2/*m*) point symmetry and forms chains along the *c*-axis (Figs. 2c, 3a). Although it is related to an icosahedron, it is better viewed starting with a distorted pentagonal antiprism with its bases normal to **c**. All atoms of the antiprism (In13, 14, 17) are exo-bonded; In13 to four different In_{11} (type A), In14 to four different icosioctahedra, and In17 to two different indium triangles. The In19 atoms that cap pentagonal antiprism appear to have a fixed and virtually 50% occupancy across the stoichiometry range (54.1 (9) to 51.5 (7)%). The refined distances from In19 to In13, 14, and 17 in the capped face (2.841 (5), 2.889 (3), and 2.788 (6) Å, respectively) are short compared with those either within the antiprism (2.95–3.10 Å) or the characteristically smaller (2-center, 2-electron) values between clusters (2.88–3.05 Å), meaning that In19 is closer to the plane of the capped pentagon (compare In17). The distance to In19 in the adjacent cluster is even shorter if both are present simultaneously—2.76 (1) Å. There are many configurational possibilities in this chain in principle: 10-bonded *arachno*-, *nido*-, and *closo*-clusters if In19–In19 con-

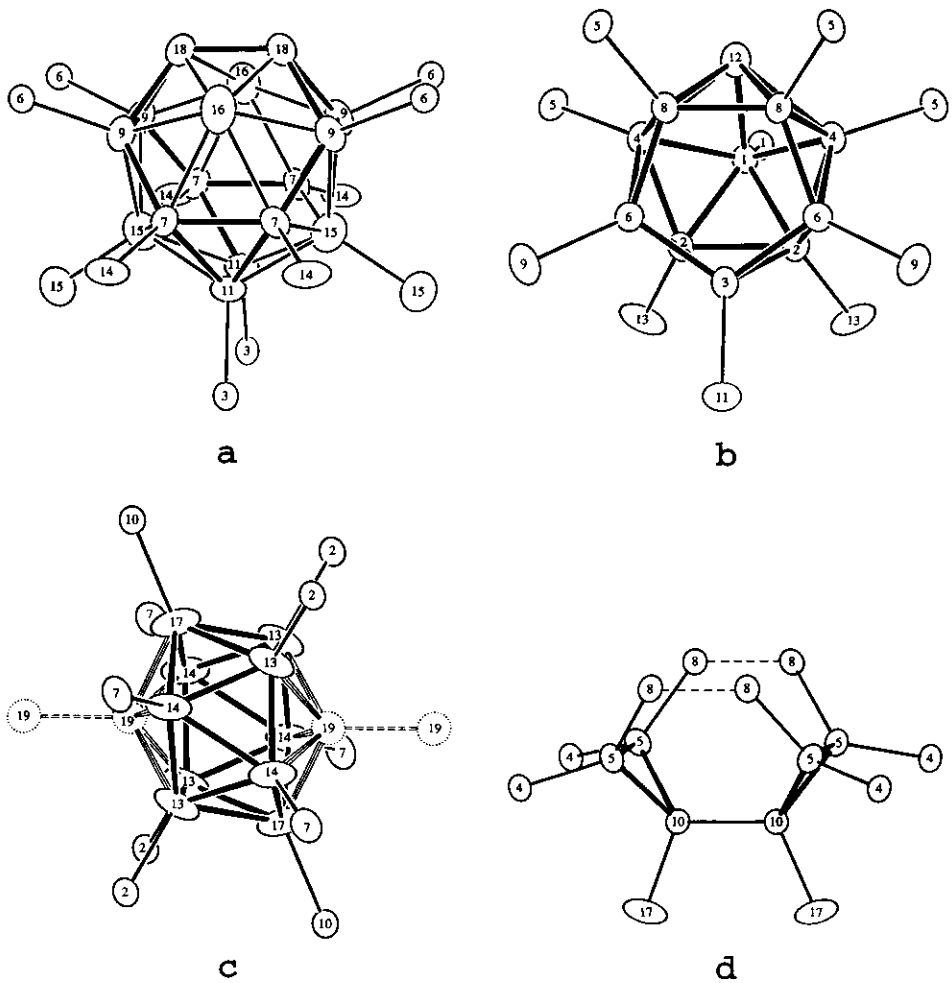

FIG. 2. The individual clusters in $Na_{15}In_{27.4}$ with exo bonds included (a) icosioctahedral In_{16}, where In15 is 100% occupied at the indium-rich limit $Na_{15}In_{27.4}$, but ~64% at the sodium-rich boundary $Na_{15}In_{27.16}$; (b) *nido*-In_{11}, type A; (c) *nido*-In_{11}, type B, in which the In19 position refines to slightly over 50% occupancy throughout the range; and (d) the pairs of indium triangles, all of four-bonded indium.

tacts are avoided, or 11-bonded *nido*- and *closo*-, and 12-bonded *closo*-clusters if In19–In19 contacts exist. These uncertainties cause complications when counting the electrons needed for the indium network bonding (below). However, the simplest arrangement may be the best—small to large regions of ordered *nido*- In_{11} units that are not directly bonded together, with long range disorder within or between chains or sheets so as to gain a nonpolar crystal.

The last building block consists of pairs of triangles, Fig. 2d. As before (6), these can also be considered as isolated 4-bonded In atoms. The pair is bonded to eight different In_{11} (A) and two In_{11} (B). The dashed

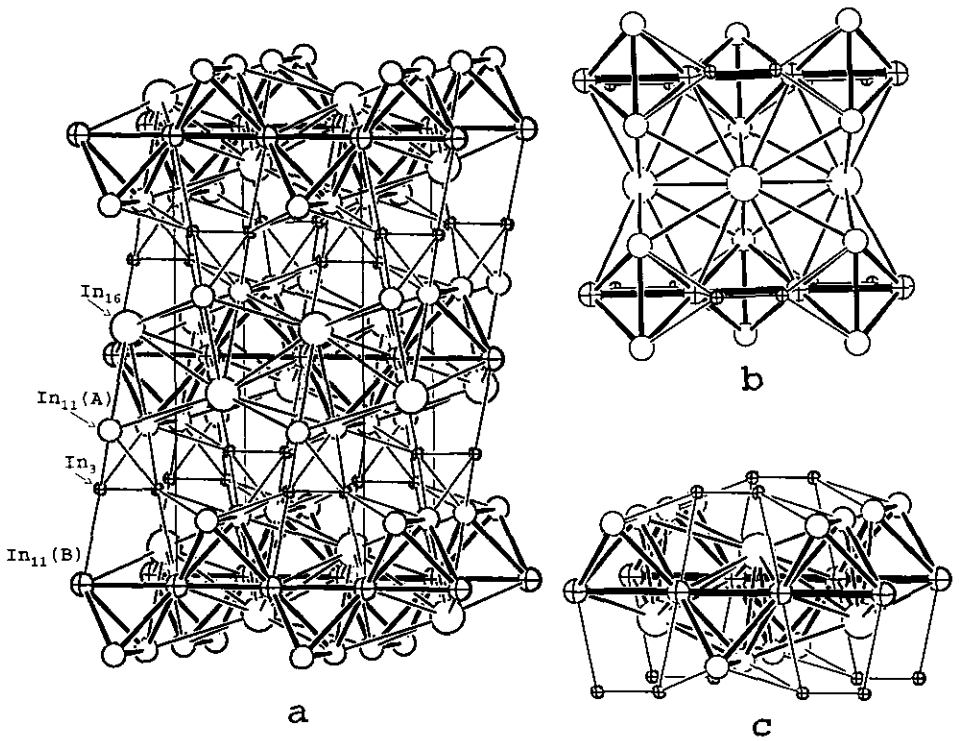

FIG. 3. (a) A view of the indium sublattice in $Na_{15}In_{27.4}$ in which large, medium, and medium crossed circles represent In_{16}, In_{11} (A), and In_{11} (B) clusters, respectively, and small crossed circles, the In_3 units. The orientation is the same as in Fig. 1; (b) a [010] view of a portion of the cluster layers in (a). The tetrahedral arrays of 2 In_{11} (A) and 2 In_{11} (B) clusters are emphasized; and (C) the same unit viewed slightly off [100].

lines in Fig. 2d between pairs of exo In8 atoms represent edges of two different In_{11} (A), Fig. 2b.

Figure 3a shows the connectivity between the cluster building blocks more clearly and in the same orientation as Fig. 1. Large circles now represent In_{16} clusters, medium circles In_{11} (A), medium crossed circles In_{11} (B), and small crossed circles, the positions of each of the In_3 units. The structure is seen to contain identical layers normal to **b**, each consisting of interconnected zig-zag chains of alternating cluster types parallel to the *c*-axis. One layer is shown in two views in Fig. 3b and 3c. One chain is constructed of interbonded 16-vertex clusters, and the second chain is formed from tetrahedra (heavier outline) of In_{11} clusters, two each of A and B. These tetrahedra alternate in their orientation along the chain, the shared corners being the type-B units. Each layer can also be constructed from pairs of levels along **b**, as seen in profile in Fig. 3c. Each level consists of squares of the 16-vertex clusters, centered by the tetrahedron of In_{11} clusters (or vice versa), and the two levels are shifted from each other by half the square's edge or, in other words, by **c**/2.

At this point, a comparison of the structures of $Na_{15}In_{27.4}$ and the recently reported $Na_7In_{11.8}$ (6) is appropriate. The indium network of the latter contains most of the same building blocks as the present case, namely,

closo-In_{16} (although 8-bonded), *nido*-In_{11} (type A only), and pairs of In_3 triangles. These also form layers that are equivalent to a single level of the double layer in $Na_{15}In_{27.4}$, Fig. 3c. In other words, the nearly tetragonal layers in $Na_{15}In_{27.4}$ can be viewed as double layers formed by the condensation of two single layers from $Na_7In_{11.8}$. The pattern of intra- and interlevel bonding in the two structures is the same. The bonding within the layers in both is mainly through direct intercluster bonds as well as via some In_{11}–In_3 interactions. The separate layers in both are bonded together only by pairs of In_3 triangles or, in other words, via isolated indium atoms.

All sodium atoms except Na1, 4, 14 cap triangular faces of the various polyhedra. The same type of positioning of the alkali metals is seen in both K_8In_{11} (12) and $Na_7In_{11.8}$ (6). The Na1 cation is centered in the icosioctahedron, while Na4 and Na14 center the tetrahedral holes formed by four In_{11}, and three In_{11} and pairs of triangles, respectively.

Na_2In

The final positional and thermal parameters and nearest neighbor distances are given in Tables IV and V, respectively. The prototype Na_2Tl structure discussed in detail before by Hansen and Smith (10) contains isolated, deformed Tl_4 clusters (C_2 point symmetry) surrounded by sodium atoms above all faces, edges and vertices of the cluster. Each sodium atom is shared by two or three tetrahedra. The In–In distances (3.066 (2)–3.152 (1) Å) are close to other intracluster bonding distances. The shortest intercluster distance is 5.393 (1) Å.

TABLE IV

POSITIONAL PARAMETERS AND B_{eq} FOR Na_2In

Atom	Posn.	*x*	*y*	*z*	B_{eq}
In1	8*c*	0.28762(6)	0.04329(8)	0.12622(7)	2.13(3)
In2	8*c*	0.05297(7)	0.67350(10)	0.52604(7)	2.98(4)
Na1	4*a*	0.0659(5)	0	0	3.3(3)
Na2	4*b*	0	0.5897(7)	1/4	3.6(3)
Na3	8*c*	0.3020(4)	0.1963(5)	0.4181(5)	4.0(3)
Na4	8*c*	0.1219(3)	0.2749(5)	0.2077(4)	3.5(2)
Na5	8*c*	0.3625(4)	0.4131(6)	0.1673(5)	4.1(3)

TABLE V

DISTANCES OF NEAREST NEIGHBORS ABOUT EACH ATOM IN Na_2In

In1		Na1		Na3		Na5	
In1	3.066(2)	2 In1	3.434(6)	In1	3.349(5)	In1	3.399(5)
In2	3.068(1)	2 In2	3.336(3)	In1	3.582(5)	In1	3.462(5)
In2	*3.152(1)*	2 Na3	*3.389(6)*	*In1*	*3.695(5)*	*In2*	*3.320(5)*
Na1	3.434(6)	2 Na4	3.532(5)	In2	3.696(5)	In2	4.180(6)
Na2	3.309(1)	2 Na5	3.521(8)	In2	3.707(6)	Na1	3.521(8)
Na3	3.349(5)	2 Na5	4.110(6)	Na1	3.389(6)	Na1	4.110(6)
Na3	3.582(5)			Na2	3.510(6)	Na2	3.570(7)
Na3	3.695(5)			Na3	3.97(1)	Na3	3.531(7)
Na4	3.318(5)			Na4	3.582(7)	Na3	3.616(7)
Na4	*3.222(5)*			*Na4*	*3.575(7)*	*Na3*	*3.837(8)*
Na5	3.399(5)			Na4	4.143(7)	Na4	3.526(7)
Na5	3.462(5)			Na5	3.531(7)	Na4	3.582(7)
				Na5	3.616(7)	Na5	4.22(1)
				Na5	3.837(8)	Na5	4.28(1)

In2		Na2		Na4	
In1	3.068(1)	2 In1	3.309(1)	In1	3.318(5)
In1	3.152(1)	2 In2	3.410(2)	In1	3.222(5)
In2	3.127(2)	2 In2	3.590(4)	In2	3.306(5)
Na1	3.336(3)	2 Na3	3.510(6)	In2	3.263(5)
Na2	3.410(2)	2 Na4	3.292(7)	Na1	3.532(5)
Na2	3.590(4)	2 Na5	3.570(7)	Na2	3.292(7)
Na3	3.696(6)			Na3	3.582(7)
Na3	3.707(6)			Na3	3.575(7)
Na4	3.306(5)			Na4	3.52(1)
Na4	3.263(5)			Na5	3.526(7)
Na5	3.320(5)			Na5	3.582(7)
Na5	4.180(6)				

Properties

The resistivities of the $Na_{15}In_{27.5}$ and Na_2In are both linear with the temperature over 130–295°C and indicate metallic behavior. The resistivities at 295 K are about 290 and 270 $\mu\Omega$-cm with coefficients of +0.26 and +0.27%K^{-1}, respectively, characteristic of "poor metals." These are comparable to ρ_{295} ~540 $\mu\Omega$-cm for the metallic $Na_7In_{11.8}$ and a ρ_{748} maximum of ~180 $\mu\Omega$-cm for a liquid Na–In mixture at ~60 at.% Na (13). It should be noted that absolute values of resistivities determined by the

"Q" method may be accurate only within a factor of three, but the temperature coefficients should be quite reliable.

Magnetic measurements gave temperature-independent susceptibilities for $Na_{15}In_{27.5}$ and Na_2In of $-(12.0 - 13.0) \times 10^{-4}$ and $-(0.4 - 0.5) \times 10^{-4}$ emu/mole, respectively, over 25–295 K. Two types of diamagnetic corrections are appropriate. Those for the Na^+ and In^{3+} ion cores total -6.0×10^{-4} emu/mole for $Na_{15}In_{27.5}$ and -0.3×10^{-4} emu/mole for Na_2In. As before (6,12), correction for the Larmor precession of the electron pair in each cluster orbital (Langevin contribution) is necessary. For r_{ave}, we averaged the appropriate distances from the center of each cluster to the middle of the different types of In–In edges on its surface. This gave 2.4 Å for the In_{11} clusters, 3.1 Å for the icosioctahedron, and 1.2 Å for the tetrahedron and, thence, -4.2, -9.8, and -0.5 ($\times 10^{-4}$) emu/mole-cluster, respectively. Based on the proportions of each cluster per formula unit, the total Larmor corrections become $\chi_L = -[(1.5 \times (4.2) + 0.5 \times (9.8)] \times 10^{-4} = -11.2 \times 10^{-4}$ emu/mole for $Na_{15}In_{27.4}$ and $\chi_L = -0.25(0.5) \times 10^{-4} = -0.12 \times 10^{-4}$ emu/mole for Na_2In. Combination of these, the ion core values, and the measured susceptibilities provides $\chi_M = +(4.2 - 5.2) \times 10^{-4}$ emu/mole for $Na_{15}In_{27.5}$ and essentially zero (-0.08 to $+0.02 \times 10^{-4}$ emu/mole) for Na_2In. We note here that the molar susceptibility of the isostructural Na_2Tl, -0.03×10^{-4} emu/mole [at 50 to -300 K (14) after similar corrections] is remarkably close to the Na_2In result. All of the diamagnetic corrections are somewhat approximate, and the χ_M results would probably be slightly more positive if corrections for the valence electrons in the $5s^2$ pairs or the intercluster bonds were included. The Langevin correction is probably less than necessary as well. The results are as they stand consistent with small Pauli paramagnetic terms, as also observed early for $Na_7In_{11.8}$ and K_8In_{11}.

Electronic Structure

$Na_{15}In_{27.4}$

Extended-Hückel MO calculations were performed on the separate 12-bonded *closo*-In_{16}, the 10-bonded *nido*-In_{11} (type A), different possibilities for the type-B In_{11} and the observed arrangement of a pair of *nido*-In_{11} (type A) clusters about one In_{16} cluster, all with the observed configurations. The procedures and parameters are described in detail elsewhere (6). The indium atoms in the pairs of triangles (Fig. 2d) were treated as isolated four-bonded atoms following our earlier investigation.

In_{16}. We have earlier shown that 8-bonded *closo*-In_{16} has 18 bonding skeletal orbitals below a 2.5-eV gap and thus requires $2n + 4 = 36$ electrons rather than the usual $2n + 2$ by Wade's rule (15). (This is a standard exception (16).) The eight exo-bonds serve to lower the local charge on the cluster from -20 to -12. The 12-bonded *closo*-In_{16} in the present structure has the same electronic requirements for the skeletal bonding and a gap of ~2.8 eV, but the closed shell charge is further decreased to -8 by four more exo-bonds. Combinations of the four lone pairs on the atoms without exo-bonds (In16, 18) form the cluster HOMO, as expected (Fig. 4). These orbitals are mainly *p*-type and are directed radially outward.

About 35% of the In15 atoms in In_{16} are missing at the indium poor limit (Experimental Section), meaning that the zig-zag chain of these is interrupted (Fig. 2a). Calculations on the 11-bonded *nido*- and 10-bonded *arachno*-clusters so formed indicated no change in the skeletal bonding requirements, $2n + 6$ for *nido* and $2n + 8$ for *arachno*. Unless the absences are correlated, there will also be In_{16} clusters in which the In15 atoms have no exo-bonds, rather only lone pairs. Calculations on such species showed that these lone pairs remain filled (although at higher energy) despite some antibonding interactions with the sur-

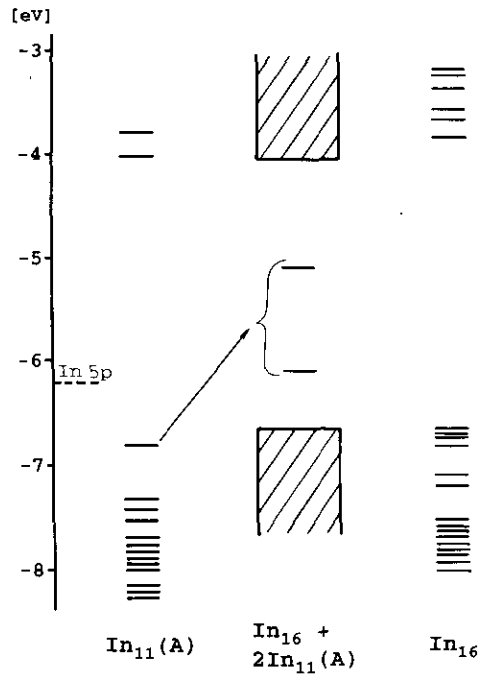

FIG. 4. The results near the valence gap from EHMO calculations for In_{11} (A) (left), In_{16} (right), and the result of the nonbonding interactions between 2 In_{11} (A) In_{16} (center). Hatched areas denote the region of unchanged M.O. energies. (Three pairs of In_{16} levels are not separable on this scale.)

rounding six exo-bonds. In other words, the In15 absences do not alter electron requirements of these clusters.

In_{11}(type A). This cluster was calculated to have 13 skeletal bonding orbitals, as expected. The HOMO is a pure lone pair on In12, the only atom without an exo-bond, that points radially outward and lies about 0.5 eV above the next bonding orbital (Fig. 4 left). Again, π^* interactions with the five neighboring exo-bonds are responsible for the higher energy.

In_{11}(type B). As discussed earlier, half-occupancy of the In19 site (Fig. 2c) leads to several possible icosahedra derivatives. Calculations were performed on all possible species. The number of skeletal bonding orbitals for all of these is 13 but the numbers of exo-bond orbitals and of filled lone pairs are different and depend upon whether the In19 atom occupancies are correlated or not. When one In19 lacks an exo-bond, the lone pair on this atom is the HOMO and lies nearly 0.8 eV above the next bonding orbital in the same cluster. This difference is relatively great because In19 lies only ~1.3 Å above the plane defined by In13, 14, 17, while In12 in the type-A cluster is ~2.0 Å above the In1, 4, 8 plane, which affords weaker antibonding interactions between the lone pair and the neighboring exo-bonds. If a single cluster lacks two exo-bonds at In19, the lone pair combinations give rise to one antibonding and one bonding molecular orbitals.

Intercluster interactions. Although the structure is built of macrolayers interconnected by isolated indium atoms, Fig. 3a, significant interactions appear possible between In_{16} in one layer and the two *nido*-In_{11} (type A) units in the next layer, similar to an effect seen in $Na_7In_{11.8}$. The arrangement here is such that each In12 in the paired *nido* icosahedra approximately caps an In16–In18–In18 triangular face in the nearest icosioctahedron. The lone pair on In12 lies almost normal to that triangular face, while the lone pairs on In16 and In18 are directed radially outward from the icosioctahedron. The distances from In12 to In16 (4.032 (4) Å) and In18 (4.152 (3) Å) are quiate long relative to "bonding" distances (2.9–3.5 Å), but still in a range to afford some repulsive interactions. Extended-Hückel MO calculations were therefore also performed on the observed In_{16}–$2In_{11}$ configuration. As shown in the center of Fig. 4, one combination of In12 lone pairs becomes antibonding and presumably empty while the second falls in the nonbonding region (~0.5 eV above the highest bonding and ~1.0 eV below the lowest antibonding orbitals) where it could be either filled or empty. This means that either every or every other *nido*-In_{11} (A) has an empty lone pair orbital on the In12 atom.

The same arrangement of 10-bonded

nido-In_{11} around In_{16} clusters occurs in $Na_7In_{11.8}$, but there the equivalent intercluster In–In distances are shorter—3.872 (6) and 4.099 (5) Å—and the lone pairs of all nearest icosahedra are pushed up in energy and emptied.

Na_2In

The tetrahedron is considered a nido-unit resulting from a removal of a threefold vertex from a closo-trigonal bipyramid. The In_4 units then have $2n + 4 = 12$ skeletal electrons according to the Wade's rules (15), giving $(Na^+)_8In_4^{8-}$ either in the extreme of electron transfer or, better, by conventional oxidation state assignments.

Electron Count

$Na_{15}In_{27.4}$. The number of electrons needed is somewhat less than that available, and the compound is electron-rich. Each unit cell contains four icosioctahedra, eight type-A and four type-B icosahedra, and 24 isolated, 4-bonded indium atoms. We also take into account the effects of fractional occupancies on the cluster requirements and of the stoichiometry range of the phase relative to the electrons available. The electron requirements for each unit and the total are as follows:

		skeletal	exo	lone pair	Σ, ea	Σ/unit cell min.	Σ/unit cell max.
$4In_{16}$		36	12	8	56	224	224
$8In_{11}$ (A)	min	26	10	0	36	288	
	max	26	10	1	37		296
$4In_{11}$ (B)	min	26	11	0	37	148	
	max	26	10	2	38		152
$24In_1$					4	96	96
closed shell total						756	768
available at $Na_{15}In_{27.54}$ limit						781	781
difference						+25	+13
available at $Na_{15}In_{27.16}$ limit						772	772
difference (excess)						+16	+ 4

The above numbers need some further comment. The In_{16} cluster in $Na_{15}In_{27.16}$ may have one (even two) In15 atom(s) missing at the indium-poor limit, but then the corresponding In15 atom/atoms on the adjacent units In_{16} will have stable lone pairs. These we can formally count as split between the two clusters, which means an occupancy-independent contribution from these units to the overall sum. The only case where this number can change is if the In15 atom from the second cluster is also missing so that a lone pair orbital is not available, but this seems less unlikely.

All *nido*-In_{11} (type A) may have an empty lone pair orbital on In12 because of nonbonded interactions with In_{16} (Fig. 4). Such an arrangement will lead to the minimum number of required electrons per cluster, 36. If every other cluster has this orbital empty, the maximum number of electrons per cluster is 37. The most complicated case is the electron count for type-B icosahedra since the number of electrons needed per cluster depends upon whether the 50% of the In19 present are exo-bonded or not. The lower limit (26 skeletal +11 for exo-bonds) is reached when all In19 atoms are exo-bonded, which means the local order gives pairs. This may not be very likely. The upper limit is reached when all clusters are *nido*-species, and none of them has In19 with an exo-bond. The real count could be anywhere between those two limits, although, as noted before, the last seems more probable.

Taking into account that every indium atom provides three valence electrons and every sodium atom one, the number of available electrons per cell ($Z = 8$) are 781 and 772 for $Na_{15}In_{27.54}$ and $Na_{15}In_{27.16}$, respectively, presuming the refined compositions are correct. The excess of electrons falls in the range of +13 to +25 (1.7–3.2%) at the former, indium-rich limit to +4 to +16 (0.5–2.0%) at the most reduced. In each case, our reasoning on uncertain electronic requirements favor the larger need and thence the smaller excess. If the maximum number of required electrons is correct, a 50% occupancy of the In15 site (rather than the 64% observed) would give

a Zintl phase at the indium-poor limit. We are remarkably close to that point already, illustrating again the apparent drive to achieve a closed shell configuration even if this requires such a complicated structure.

Na_2In. We count the electrons for the formula Na_8In_4 and one In_4 tetrahedron. Those needed for skeletal bonding and lone pairs total $12 + 4 \times 2 = 20$. The number available is also 20 ($= 4 \times 3 + 8 \times 1$), suggesting that Na_2In could be semiconducting if the electron transfer from sodium to the In_4 unit is complete or, better, that the valence and conduction bands do not overlap. Alternatively, six 2-e bonds can be ascribed to the edges of the In_4 tetrahedron. The observed In–In bond distances, 3.066 (2) to 3.152 (1) Å (3.106 Å ave.) might seem long relative to the two-center two-electron intercluster bonds in the network structures, 2.85 to 3.02 Å, or the standard single bond, 2.84 Å (17). This does not necessarily imply delocalization of some bonding electrons out onto sodium. Bent bonds (reduced overlap) is one consideration, and charge repulsion is another. The comparative Sn_4^{4-} in β-NaSn exhibits edge distances of 2.967 (2) Å (18) relative to a metallic single bond distance of 2.842 and 2.80 Å in gray tin (17). Charge repulsion effects of 0.15–0.20 Å have been estimated in lengthening Tt_2^{4-} dimers (19) (Tt = tetregen).

Physical Properties

The poor but metal-like conductivity characteristics of $Na_{15}In_{27.5}$ as well as its small Pauli-like magnetic susceptibility are nicely consistent with the foregoing electronic expectations for this phase. A few excess electrons in this complex arrangement should not detract from the considerable importance of covalent In–In bonding in and between the clusters. The term "metallic Zintl phase" (19) is again apt. The Na_2In phase is substantially diamagnetic, but a weak metallic conductivity contradicts the expectation from straightforward electron counting. Some small back donation from the In_4 anion with a formal 8– charge onto the sodium cations (of the same symmetry) and into the conduction band would not be surprising. A useful comparison can be made with the structure and properties of β-NaSn. Calculations based on an augmented spherical wave method involving both Na and Sn states place the Fermi level in a gap between broadened cluster (plus sodium) valence and sodium-plus-cluster conduction bands, so that the compound is predicted to be a semiconductor (20). Conductivity measurements show a contrary metallic property (21). This mismatch is not substantial and could be explained by some modest broadening of the calculated valence (cluster dominated) and conduction (Na) bands to give a small density of states at E_F. Again, this would in no way detract from the significance or importance of the cluster bonding.

Phase Diagram

Figure 5 shows our proposal for a revised phase diagram for the In–Na system. We have chosen as a starting model the diagram reported by Thümmel and Klemm in (4) and have kept all of the reported points and the resulting liquidus curve. Their data for the two eutectics and the NaIn peritectic are substantially the same as in the most recent compilation where the In(Na) liquidus end is also described (1, 2). The following have been changed: the congruently melting composition of about Na_5In_8 is corrected to $Na_7In_{11.8}$, and the neighboring $Na_{15}In_{27.5}$ is added. Each is somewhat nonstoichiometric but not sufficiently so for this diagram. The eutectic transformations stop at $Na_{15}In_{27.5}$ and Na_2In although they were observed beyond these compositions in thermal analysis (3, 4), not too surpris-

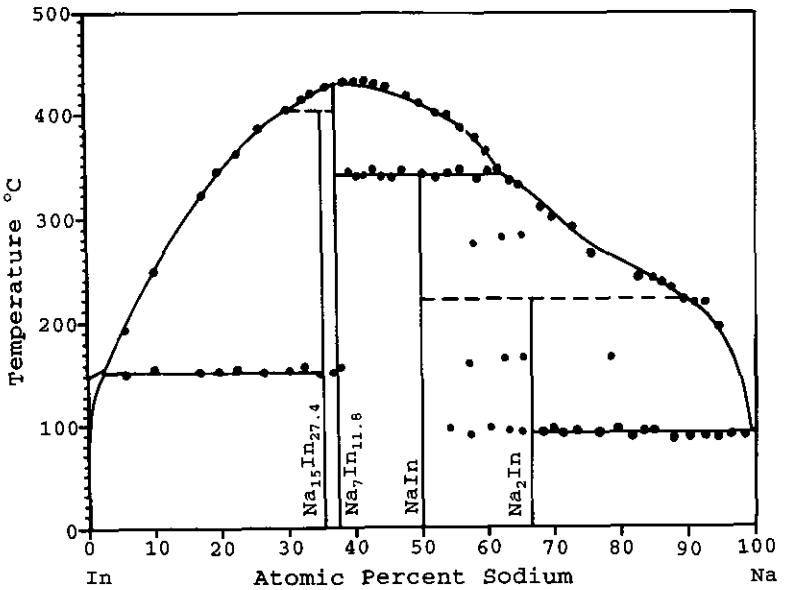

FIG. 5. The revised In–Na phase diagram based on the cooling curve results of Thümmel and Klemm (4) accepted fixed point data (1, 2), and the synthetic and structural studies of $Na_7In_{11.8}$ (6), $Na_{15}In_{27.4}$, and Na_2In. The peritectic temperature for $Na_{15}In_{27.4}$ is arbitrary, while that for Na_2In is estimated from the liquidus behavior and a few equilibration results (see text).

ingly. The peritectic temperature for $Na_{15}In_{27.5}$ is placed somewhat arbitrarily.

The character and placement of the sodium-richest phase has needed some attention. Thümmel and Klemm (4) correctly assessed the composition as near Na_2In ("around about $Na_{2.3}In$") but concluded from differential thermal measurements that the phase was stable only between ~285°C and ~165°C. They are the only investigators to have reported thermal effects in the latter region (Fig. 5). On the other hand, Lamprecht and Crowther (3) concluded that the phase was Na_3In, largely on the basis of an analysis of crystalline product supposedly isolated from excess sodium. In addition, they appear to have confused a peritectic decomposition of their Na_3In with the sodium-rich eutectic at 96°C. Our equilibration and X-ray studies establish that the phase is Na_2In and that it is stable from room temperature (or below) to somewhere between 180 and 240°C where a peritectic decomposition to NaIn(s) and Na(In)(ℓ) takes place. Our placement of the fixed point near 220°C was guided by the behavior of the reported liquidus data near 90% Na.

Acknowledgments

We are indebted to J. Shinar for the use of the Q apparatus, and to J. E. Ostensen and D. J. Finnemore for the magnetic data.

References

1. "Binary Alloy Phase Diagrams," 2nd ed., Vol. 3, p. 2261, American Society for Metals, Metals Park, Ohio 44073 (1990).
2. S. LAROSE AND A. D. PELTON, *Phase Equilib.* **12,** 371 (1991).
3. G. J. LAMPRECHT AND P. J. CROWTHER, *J. Inorg. Nucl. Chem.* **31,** 925 (1969).
4. THÜMMEL AND W. KLEMM, *Z. Anorg. Allg. Chem.* **44,** 376 (1970).

5. E. ZINTL AND S. NEUMAYR, *Z. Phys. Chem.* **B20,** 270 (1933).
6. S. C. SEVOV AND J. D. CORBETT, *Inorg. Chem.* **31,** 1895 (1992).
7. TEXAN, Version 6.0 package, Molecular Structure Corp., The Woodlands, TX, 1990.
8. G. M. SHELDRICK, SHELX-86, Universität Göttingen, BRD (1986).
9. N. WALKER AND D. STUART, *Acta Crystallogr. Sect. A* **39,** 158 (1983).
10. D. A. HANSEN AND J. F. SMITH, *Acta Crystallogr.* **22,** 836 (1967).
11. J. SHINAR, B. DEHNER, B. J. BEAUDRY, AND D. T. PETERSON, *Phys. Rev. B* **37,** 2066 (1988).
12. S. C. SEVOV AND J. D. CORBETT, *Inorg. Chem.* **30,** 4875 (1991).
13. C. VAN DER MAREL, E. P. BRAUNDERBURG, AND W. J. VAN DER LUGT, *J. Phys. F: Met. Phys.* **8,** L273 (1978).
14. J. D. GREINER, D. A. HANSEN, AND J. F. SMITH, *J. Less-Common Met.* **19,** 23 (1969).
15. K. WADE, *Adv. Inorg. Chem. Radiochem.* **18,** 1 (1976).
16. P. W. FOWLER, *Polyhedron* **4,** 2051 (1985).
17. L. PAULING, "The Nature of the Chemical Bond," 3rd ed., pp. 400, 403, Cornell Univ. Press, Ithaca, New York (1960).
18. W. MÜLLER AND K. VOLK, *Z. Naturforsch. B* **32,** 709 (1977).
19. R. NESPER, *Prog. Solid State Chem.* **20,** 1 (1990).
20. F. SPRINGELKAMP, R. A. DE GROOT, W. GEERTSMA, W. VAN DER LUGT, AND F. M. MUELLER, *Phys. Rev. B* **32,** 2319 (1985).
21. R. NESPER, private communication (1990).